Isomerization of Propylene Oxide. Quantum Chemical Calculations and Kinetic Modeling

Faina Dubnikova and Assa Lifshitz*

Department of Physical Chemistry, The Hebrew University of Jerusalem, Jerusalem 91904, Israel

Received: December 23, 1999; In Final Form: February 28, 2000

The mechanism of propylene oxide isomerization, to yield four isomerization products, was calculated by the B3LYP/cc-pVDZ method. Coupled cluster CCSD(T) calculations for the reactant, products, transition states, and intermediates were carried out to estimate the activation energies. The vibrational frequencies, calculated using B3LYP method, were used to estimate transition state theory frequency factors. The potential energy profiles of the isomerization of propylene oxide to acetone, propanal, and allyl alcohol contain one transition state each, indicating that these reactions proceed via concerted mechanisms with simultaneous C−O bond rupture and 1,2- or 1,4-H-atom shift. The potential energy surface of the isomerization of propylene oxide to methyl vinyl ether contains three transition states and two intermediates. The initial step of the process is a C−C bond cleavage with a relatively low barrier. The first intermediate has a trans structure, and the second intermediate on the surface has a cis structure. The cis → trans isomerization is a key issue in the isomerization process. The last stage is a 1,4-H-atom shift. The rate constants calculated at the coupled cluster CCSD(T)/cc-pVDZ//B3LYP/cc-pVDZ level of the theory show a fair agreement with the experimental values.

I. Introduction

Propylene oxide (methyloxiran) is a three-membered ring in which an oxygen atom replaces a $-CH_2$ group in methylcyclopropane. The ring has a strain energy of ∼27 kcal/mol, and it is kinetically unstable. The thermal reactions of propylene oxide were studied experimentally at both low[1] (654−717 K) and high temperatures[2] (850−1250 K) using the single-pulse shock tube technique. This is in contrast to ethylene oxide, which has only one isomerization channel (ethylene oxide → acetaldehyde), propylene oxide, which is an asymmetrical molecule that isomerizes to four isomerization products when it is elevated to high temperatures. The isomerization products are acetone, propanal, methyl vinyl ether, and allyl alcohol.

It has been suggested that the isomerization channels for propanal, acetone, and allyl alcohol involve the rupture of one of the two nonequivalent C−O bonds, followed by 1,2-H-atom migration for propanal and acetone and 1,4-H-atom migration for allyl alcohol. The channel for the production of methyl vinyl ether is associated with the rupture of the C−C bond, followed by 1,4-H-atom migration. The assumption that allyl alcohol and methyl vinyl ether were indeed formed by unimolecular isomerizations, and not by free radical reactions such as $CH_3O^{\bullet} + CH_2{=}CH^{\bullet} \rightarrow CH_2{=}CH{-}O{-}CH_3$, was verified by isotope labeling experiments.[2]

In view of the fact that propylene oxide is less stable than propanal by ∼23 kcal/mol and is less stable than acetone by 31 kcal/mol, these two isomers are produced in a thermally excited state, and decomposition of these two products from the thermally excited state occurs as a competition to de-excitation.[2]

We are not aware of any quantum chemical calculations on the homogeneous structural isomerization of propylene oxide. Ab initio calculations on the geometrical isomerization of ethylene oxide and its thermal fragmentation have been reported.[3−6] The heterogeneous metal and metal oxide catalyzed isomerization of propylene oxide using a semiempirical method has been also reported.[7] Also, there are two recent publications on ethylene oxide[8] and propylene oxide[9] dissociations. They were done at high-level ab initio calculations but dealt only with ionic species for both the intermediates and the transition states.

In this investigation, the potential surfaces of the four-isomerization channels have been determined using density functional theory (DFT) and coupled cluster calculations, including both single and double substitutions with triple excitations CCSD(T). The suggested mechanisms[2] for the four-isomerization products were verified. Also, isomerization rate constants using transition state theory were calculated and compared with the experimental results. The agreement obtained is reasonably good.

II. Computational Details

All of the stationary points on the potential energy surfaces were optimized at the DFT level of the theory. We used the Becke three-parameter hybrid method[10] with the Lee−Yang−Parr correlation functional approximation (B3LYP)[11] and the Dunning correlation consistent polarized valence double-ξ (cc-pVDZ) basis set.[12,13] The higher level calculations were then carried out at these geometries.

Vibrational analyses were carried out at the same level of theory to characterize the optimized structures as local minima or transition states. The calculated vibrational frequencies and entropies (at B3LYP level) were used to evaluate preexponential factors of the reactions under consideration. All of the calculated frequencies, as well as the zero-point energies, are of harmonic oscillators. The zero-point energies were scaled by the ZPE scaling factor of 0.9806, and the entropies were scaled by the entropy scaling factor 1.0015.[14] The calculations of the intrinsic reaction coordinate (IRC) were done at the uB3LYP level of theory with mass-weighted internal coordinates to check whether the transition states under consideration connect the expected reactants and products. Only this coordinate system permits one to follow the steepest descent path.[15] We computed the IRC

10.1021/jp994485t CCC: $19.00
Published on Web 04/26/2000

path with the same basis set that was used for the stationary-point optimization.

Biradical structures on the surface of methyl vinyl ether were localized using guess wave functions, with the destruction $\alpha-\beta$ and spatial symmetries determined by the unrestricted uB3LYP method. We used an open-shell singlet approximation for the biradical structures. It should be mentioned that numerous recent studies on this issue indicate that the spin-unrestricted B3LYP method for geometry optimization of biradical transition states and intermediates, as well as for activation energies, was in reasonable agreement with the multirefence or multiconfigurational results and the available experimental data.[16−23]

The relative energies of various transition states and intermediates were evaluated further by CCSD(T). CCSD(T) calculations were performed with the frozen core approximation, using the same basis set, namely, cc-pVDZ. All of the reported relative energies include the zero-point energy correction (ZPE). The DFT and CCSD(T) computations were carried out using the Gaussian-94 program package.[24] The CASSCF(4,3) calculations were carried out using the Gamess-USA program.[25] All of the calculations were carried out on a DEC Alpha TurboLaser 8200 5/300 at the Institute of Chemistry of The Hebrew University of Jerusalem.

III. Results and Discussion

The potential energy surfaces for four isomerization pathways corresponding to the production of acetone, propanal, methyl vinyl ether, and allyl alcohol were calculated. All of the four isomerizations involve cleavage of either C−O or C−C bonds followed by H-atom migrations. The bond that is broken and the mode of H-atom migration determine which isomer is produced. The following reaction scheme provides a schematic description of the four-isomerization reactions.

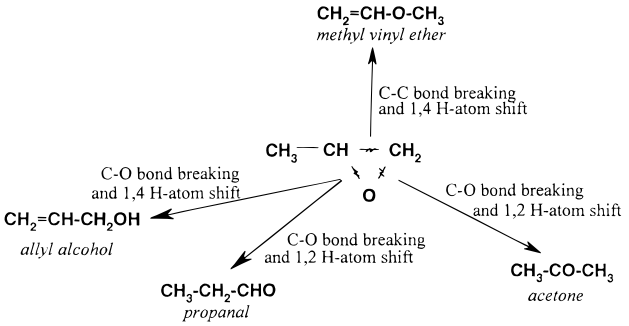

A. Acetone. The potential energy surface of the propylene oxide → acetone isomerization is shown in Figure 1. The surface contains a single transition state (TS1), which means that the isomerization proceeds via a concerted mechanism. Judging by the atom's movement of the normal mode of the imaginary frequency, the reaction coordinate is a combination of two movements, which are the $O_1C_3C_2$ angle bend and the 1,2-H-atom shift of H_3 from C_3 to C_2. The $O_1C_3C_2$ angle changes from 59.05° in the reactant to 113.28° in the transition state and to 121.76° in the product. Enlargement of the $O_1C_3C_2$ angle is accompanied by stretching of the O_1-C_2 distance from 1.434 Å in propylene oxide to 2.279 Å in TS1, which is practically bond breaking. On the other hand, the H_3 in the transition state is still closer to the original carbon atom C_3, C_3-H_3 =1.179 Å (1.100 Å in the reactant) than to the accepting carbon atom C_2, C_2-H_3 =1.932 Å (2.202 Å in the reactant). In addition, the angle $H_3C_3C_2$ has changed from 117.09° in the reactant to 93.74° in the transition state. Note that the C_3-O_1 bond in propylene oxide, which is a single bond with a distance of 1.436 Å, is shortened in the transition state (1.315 Å) toward the formation of a $C_3=O_1$ double bond in acetone with a distance of 1.214 Å. The spin contamination $<S^2>$ of the transition state is zero, indicating that the electronic structure corresponds to a closed shell singlet and not an open shell biradical. The loss of one bond by cleavage of the O_1-C_2 bond is compensated by increase in the bond order of C−O from a single bond to something between a single bond and a double bond (1.315 Å) and leaving some fractional bond order between O_1 and C_2. In addition, a bond between C_2 and H_3 begins to be formed. Altogether, there is no loss of the bond order by transition from the reactant to TS1.

The energy barrier of the transition state TS1 calculated at CCSD(T)//B3LYP/cc-pVDZ level of theory with ZPE energy correction is 54.10 kcal/mol.

B. Propanal. The potential energy surface of the propylene oxide → propanal isomerization is shown in Figure 2. This surface contains also a single transition state (TS2). Here too, the isomerization to propanal has a concerted mechanism. However, in acetone, the O_1-C_2 bond is broken and H atom migrates from C_3 to C_2, whereas in propanal, the O_1-C_3 bond is broken and H atom migrates from C_2 to C_3. The reaction coordinate is a combination of two normal modes, $O_1C_2C_3$ angle bend and 1,2-H-atom shift. The bond length O_1-C_3 changes from 1.436 Å in the reactant to 2.307 Å in the transition state TS2. The transition state TS2 is also a closed shell structure with some through-space interaction of the unpaired electron on the oxygen with the unpaired electron on C_3. The C_2-O_1 bond length is 1.308 Å, this is an intermediate length between a single and a double bond. The C_2-O_1 bond length in the reactant is 1.436 Å and the C_2-O_1 bond length in the product is 1.208 Å. The hydrogen atom H_1 is moving from C_2 to C_3, forming some σ-bond already in the transition state (H_1C_2 and H_1C_3 are 1.175 and 1.988 Å, respectively).

The energetic barrier on this surface is equal to 54.91 kcal/mol at the CCSD(T)//B3LYP/cc-pVDZ level of the theory.

C. Allyl Alcohol. The structures of the reactant, the transition state TS3, and the product on the potential energy surface of the propylene oxide → allyl alcohol isomerization are shown in Figure 3. As has been found in the previous two isomerizations, the single transition state on the surface indicates a concerted mechanism. Similar to the isomerization of propanal, the O_1-C_3 bond in the transition state TS3 is practically broken, but it is associated with a 1,4 H-atom migration from C_4 to O_1, rather than a 1,2 migration. As is indicated by the atom's movement in the normal mode of the imaginary frequency, the reaction coordinate is a combination of two movements. The main movement is a 1,4-H-atom shift, with a simultaneous rotation of the remaining methylene group $H_5C_4H_6$. The C_3-O_1 bond increases from 1.436 Å in the reactant to 1.933 Å in the transition state. However, this distance in TS3 is considerably shorter than the corresponding value of 2.307 Å in TS2. The hydrogen atom H_4, which moves from the methyl group toward the oxygen in the transition state, is somewhere in the middle between the oxygen and carbon atom C_4, with distances of C_4-H_4 = 1.368 and O_1-H_4 = 1.398 Å. Although the bond C_3-O_1 is practically broken, the transition state is a closed shell singlet, as in the previous two isomerizations, and not an open shell singlet (biradical). As in the previous two isomerizations, new fractional bonds are formed that, together with the remaining order in the C_3-O_1 bond, come to an approximate order of unity. Judging by the atomic distances, the major contribution comes

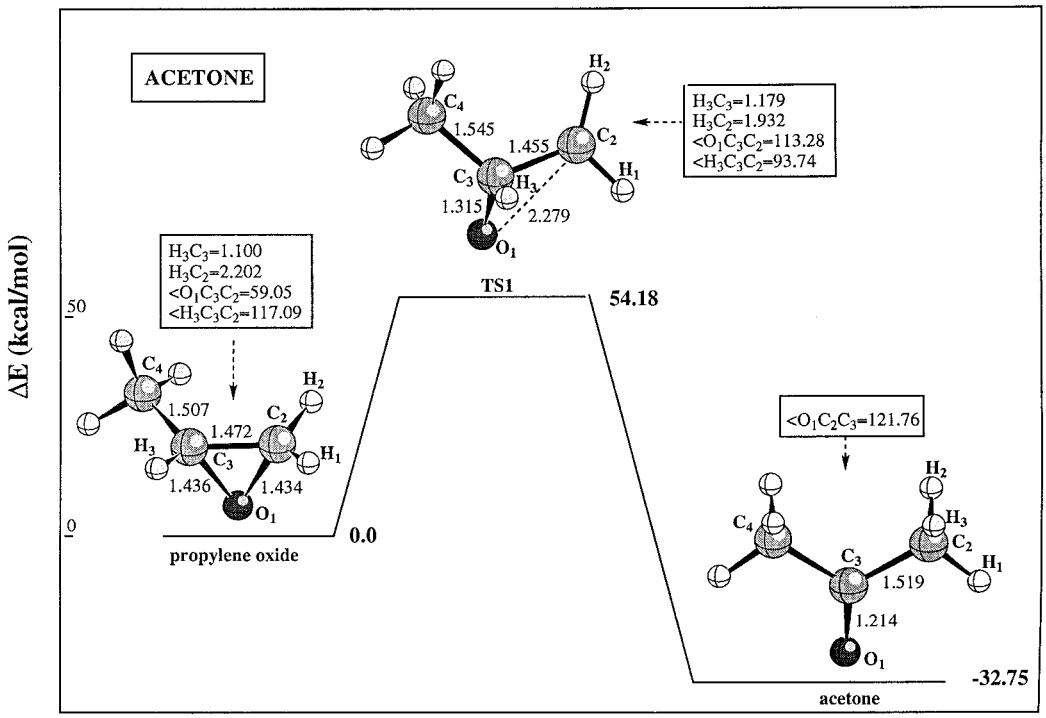

Figure 1. Potential energy profile of the propylene oxide → acetone isomerization. Relative energies (in kcal/mol) are calculated at the CCSD-(T)//B3LYP/cc-pVDZ level of theory. Distances (in Å) and angles (in degrees) are shown as calculated at the B3LYP level.

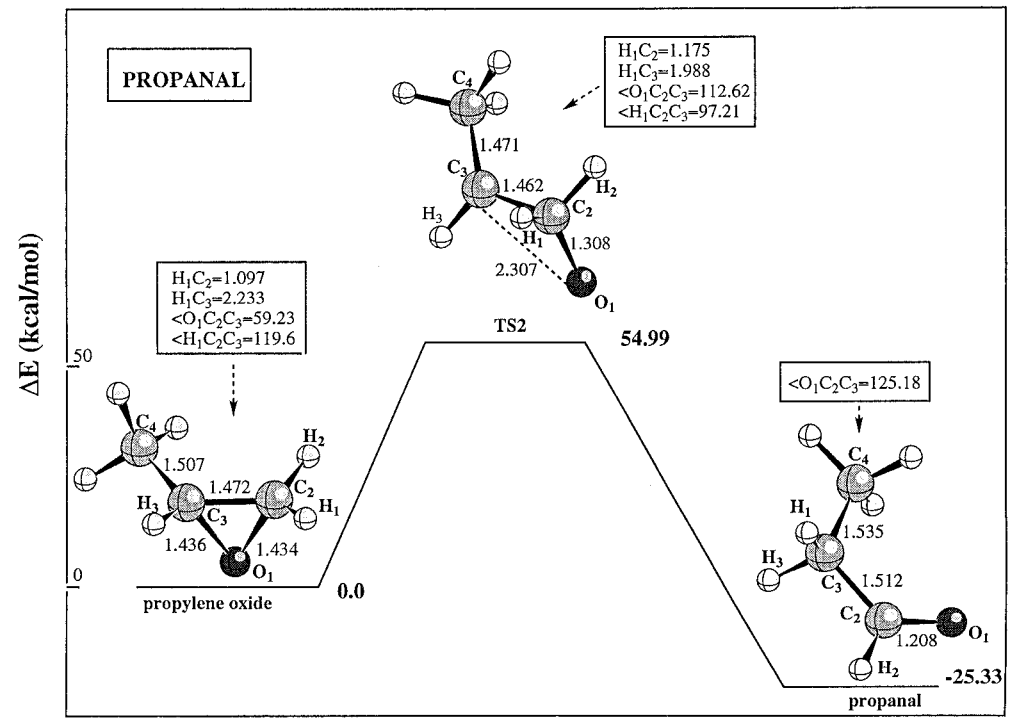

Figure 2. Potential energy profile of the propylene oxide → propanal isomerization. Relative energies (in kcal/mol) are calculated at the CCSD-(T)//B3LYP/cc-pVDZ level of theory. Distances (in Å) and angles (in degrees) are shown as calculated at the B3LYP level.

from the C_3-O_1 bonds, but the bonds C_3-C_4 and C_2-H_4 also contribute.

The energy barrier of the isomerization is 60.17 kcal/mol at the CCSD(T)//B3LYP/cc-pVDZ level of the theory.

D. Methyl Vinyl Ether. The only reaction that proceeds via a stepwise mechanism is the isomerization of propylene oxide to methyl vinyl ether. Another major difference is the breaking of the C_2-C_3 bond and not one of the C−O bonds. As can be seen in Figure 4, the potential energy surface of the propylene oxide → methyl vinyl ether isomerization involves three transition states and two intermediates. The reaction coordinate of the first stage is a $C_2O_1C_3$ angle bend combined with conrotatory double rotation of the $H_1C_2H_2$ methylene group with respect to the other two carbons and their hydrogen atoms. This leads to the formation of the intermediate INT1 via transition state TS4. The $C_2O_1C_3$ angle changes from 61.72° in propylene oxide to 110.11° in the transition state TS4 and 130.89° in INT1, and the distance C_2-C_3 changes from 1.472 Å in propylene oxide to 2.106 Å in the transition state TS4 and 2.379 Å in the intermediate. The long C_2-C_3 distance indicates that the C_2-

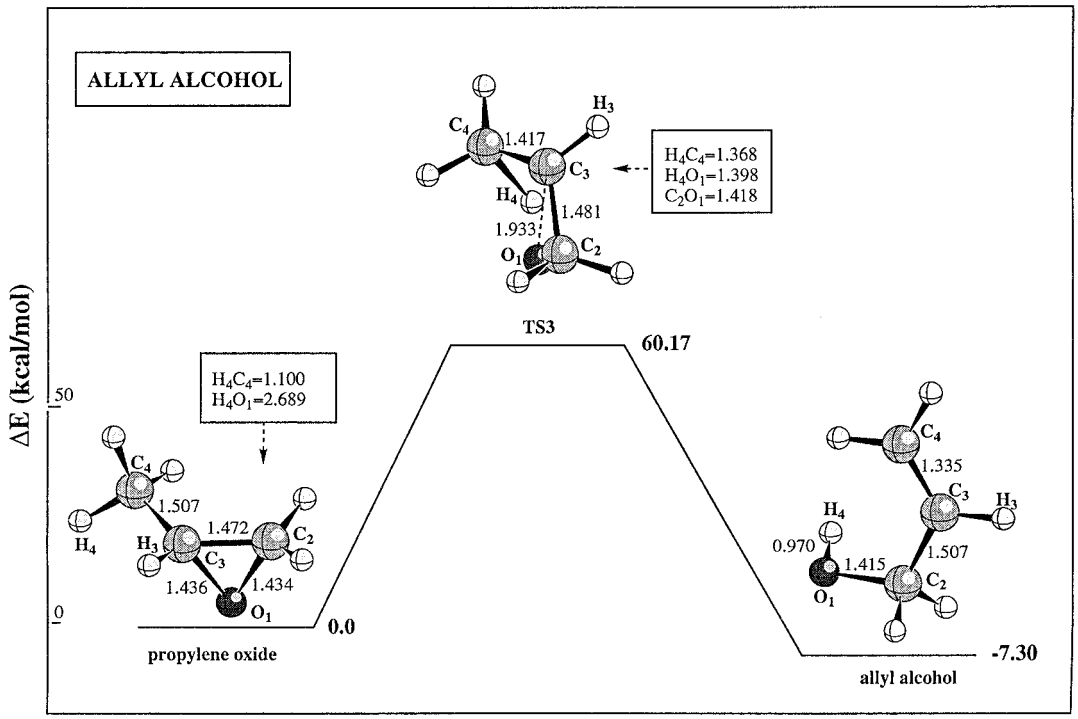

Figure 3. Potential energy profile of the propylene oxide → allyl alcohol isomerization. Relative energies (in kcal/mol) are calculated at the CCSD(T)//B3LYP/cc-pVDZ level of theory. Distances (in Å) and angles (in degrees) are shown as calculated at the B3LYP level.

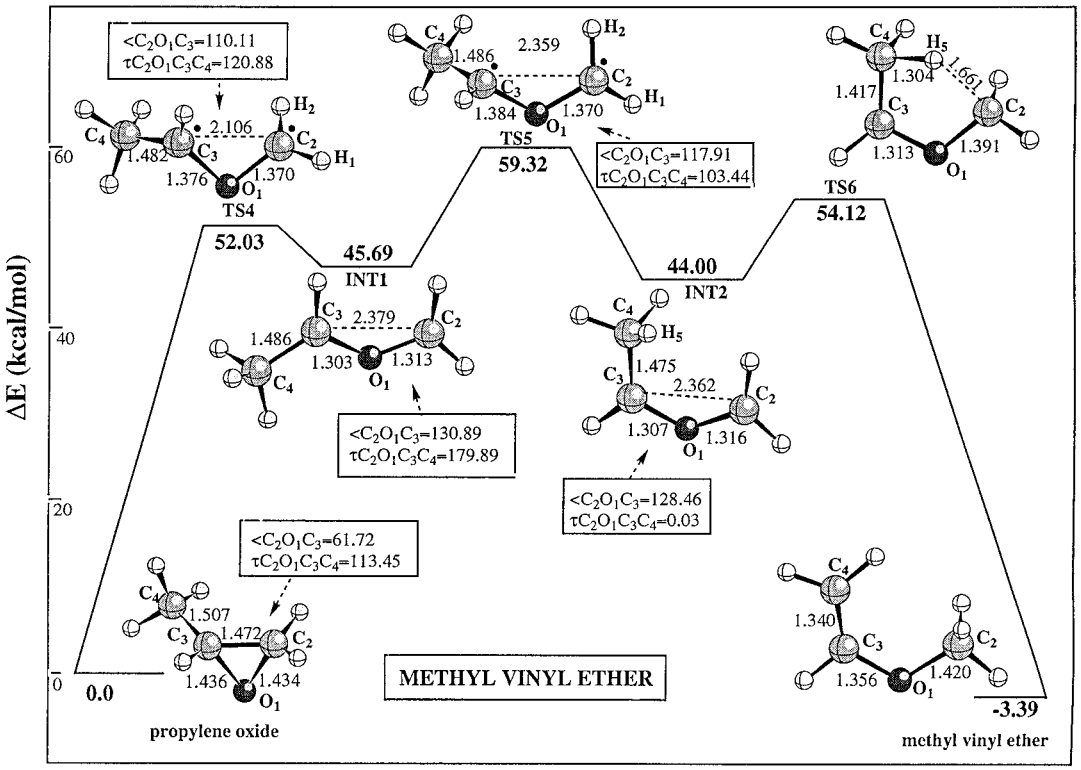

Figure 4. Potential energy profile of the propylene oxide → methyl vinyl ether isomerization. Relative energies (in kcal/mol) are calculated at the CCSD(T)//B3LYP/cc-pVDZ level of theory. Distances (in Å) and angles (in degrees) are shown as calculated at the B3LYP level. The reaction proceeds via stepwise biradical mechanism.

C_3 bond is broken already in the transition state. In contradiction to the previous isomerizations, the transition state does not have a closed shell structure and has a spin contamination of $\langle S^2 \rangle = 0.51$. The unpaired electrons on both C_2 and C_3 interact between themselves, as it is evident from the analysis of the molecular orbitals. This prevents the transition state from having a pure biradical structure.

The intermediate INT1 has a closed shell structure. The C_2-C_3 bond is completely broken with a distance of 2.379 Å, as compared to 2.106 Å in the transition state, and there is no interaction at all between C_2 and C_3. However, because the intermediate is planer with respect to all of the atoms (except for the hydrogen atoms of the methyl group), the orbital symmetry allows the spin densities on these carbon atoms to

TABLE 1: Total Energies E_{total} (in au), Zero-Point Energies, Relative Energies ΔE, Imaginary Frequencies, Entropies, and Spin Contamination for All of the Species of Propylene Oxide Isomerization, Calculated at B3LYP/cc-pVDZ and CCSD(T)/cc-pVDZ// B3LYP/cc-pVDZ Computational Levels

	B3LYP						CCSD(T)	
species	E_{total}	ΔE^b	ZPE[a]	S^d	ν^c	$<S^2>$	E_{total}	ΔE
reactant and products								
propylene oxide	−193.115 251	0.00	52.11	66.96		0.0	−192.587 392	0.0
acetone	−193.164 302	−31.90	50.99	72.24		0.0	−192.637 790	−32.75
propanal	−193.152 029	−23.62	51.53	70.81		0.0	−192.626 844	−25.33
allyl alcohol	−193.126 166	−6.87	52.09	68.78		0.0	−192.599 000	−7.30
cis-methyl vinyl ether	−193.123 809	−5.37	52.11	68.30		0.0	−192.592 793	−3.39
trans-methyl vinyl ether	−193.120 353	−3.82	51.49	73.47		0.0	−192.588 512	−1.38
transition states and intermediates								
TS1	−193.005 673	64.79	48.14	68.00	(*i* − 969)	0.0	−192.494 722	54.18
TS2	−193.016 529	57.44	47.60	68.90	(*i* − 725)	0.0	−192.493 429	54.45
TS3	−193.019 831	56.13	48.36	65.69	(*i* − 2084)	0.0	−192.485 541	60.17
TS4	−193.026 829	51.73	48.35	71.14	(*i* − 512)	0.51	−192.498 489	52.03
INT1	−193.045 115	41.56	49.66	73.17		0.0	−192.510 676	45.69
TS5	−193.022 391	54.38	48.22	70.59	(*i* − 309)	1.00	−192.486 659	59.32
INT2	−193.050 842	38.40	50.09	70.09		0.0	−192.517 277	44.00
TS6	−193.030 068	50.37	49.03	64.96	(*i* − 1204)	0.0	−192.496 237	54.12
TS7	−192.995 007	72.32	48.15	67.56	(*i* − 816)	0.0	−192.465 825	71.49
INT3	−193.060 594	32.59	50.40	71.94		0.0	−192.531 375	33.44
TS8	−193.018 598	56.85	48.31	70.42	(*i* − 1413)	0.0	−192.485 269	60.28

[a] Zero-point energies in kcal/mol. ZPE were scaled by the ZPE scaling factor, 0.9806.[14] [b] Relative energies in kcal/mol. $\Delta E = \Delta E_{total} + \Delta(\text{ZPE})$. [c] Imaginary frequencies in cm^{-1} [d] Entropies in cal/(K.mol). Entropies were scaled by the entropy scaling factor of 1.0015.[14]

interact via a lone pair of the oxygen atom. This results in the delocalization of the unpaired electrons. The interaction expresses itself by the shortening of the C_2-O_1 and C_3-O_1 bonds from 1.376 and 1.370 Å to 1.303 and 1.313 Å in the intermediate, which is the distance between a single and a double bond.

The energy barrier of the first stage of the isomerization, calculated at the coupled cluster level of the theory, is 52.03 kcal/mol. This barrier reflects a C−C bond rupture, compensated to some extent by the release of the strain energy of the ring. The barrier (which is not at the top of the surface) is smaller than the barrier of the previous three isomerizations, as they also contain H-atom migrations.

The second stage of the process is a cis−trans isomerization with respect to the O_1-C_3 bond, forming the intermediate INT2 via the transition state TS5. The structure of the intermediate INT2 is very similar to the structure of the intermediate INT1, and it is also a closed shell singlet. It also has a planer structure for all of the atoms, except the hydrogens of the methyl group, and the C−O bond lengths are also very close to the equivalent ones in INT1. The transition state TS5, on the other hand, has a full biradical character with spin contamination of 1.00 (Table 1). The biradical character of the transition state results from the loss of planarity due to the conrotatory double rotation of the $C_2H_1H_2$ methylene group with respect to the other two carbon atoms and their hydrogen atoms, which is the reaction coordinate of this step. The loss of planarity (a change from 180 to 103.4° in the dihedral angle $C_4C_3O_1C_2$) completely cancels the interaction between the unpaired electrons on C_2 and C_3 via the lone pair of the oxygen. Also, the long distance of C_2-C_3 (2.359 Å) does not allow any direct interaction between C_2 and C_3. This leaves a spin contamination of 1 in TS5. The lack of interaction between C_2 and C_3 also expresses itself by a stretch of the C_2-O_1 and C_3-O_1 bond from 1.313 and 1.303 Å to 1.370 and 1.384 Å, respectively.

The energy level of TS5 is about 14 kcal/mol above INT1, which results in a barrier of 59.32 kcal/mol with respect to propylene oxide.

The intermediate INT2, which has a cis structure, undergoes a 1,4 H_5 shift from C_4 to C_2 to produce the cis isomer of methyl vinyl ether, via transition state TS6. Owing to the 1,4 H-atom migration, the structure of the transition state resembles a five-membered ring composed of the atoms C_2, O_1, C_3, C_4, and H_5. The transition state TS6 has a closed shell structure similar to INT2, but the bond length distributions are different. In the intermediate INT2, C_2-O_1 and C_3-O_1 have bond orders of approximately 1.5 each, whereas these bonds in TS5 are C_3-O_1 and C_3-C_4. In addition, the C_4-H_5 bond in the intermediate INT2 increases to 1.304 Å, and the C_2-H_5 distance decreases to 1.661 Å. These two bonds together amount to a bond order of unity.

The energy barrier of TS6, as calculated at the CCSD(T) level of theory, is 54.12 kcal/mol above propylene oxide. This value is lower than the energy level of TS5, which is 59.32 kcal/mol. The energy level of TS5 is the highest on the potential energy surface of the propylene oxide → methyl vinyl ether isomerization, and it can be considered as the energy barrier of the isomerization.

We tried to locate a transition state leading directly from propylene oxide to INT2, which has the cis structure required to obtain the ether but were unsuccessful. On the other hand, we found another pathway from propylene oxide to methyl vinyl ether via a singlet carbene intermediate. The potential energy surface of this pathway is shown in Figure 5. The reaction coordinate of the first transition state, TS7, leads to INT3 and is a combination of two normal modes, $C_2O_1C_3$ angle bend and 1,2 H-atom shift from C_3 to C_2. As a result of the angle bend, the C_2-C_3 bond extends from a distance of 1.472 to 1.854 Å in the transition state. This distance, being less than 0.4 Å higher than the corresponding bond in propylene oxide, still preserves the three-membered ring structure to some extent. The final product of this path is a trans ether, whereas in the previous path, it is a cis isomer. However, the barrier that separates the two isomers is 3.73 kcal/mol, as calculated at the CCSD(T) level of the theory, so that they are practically in a state of equilibrium.

The energy level of transition state TS7 calculated at the CCSD(T) level of theory is 72.41 kcal/mol, which is much

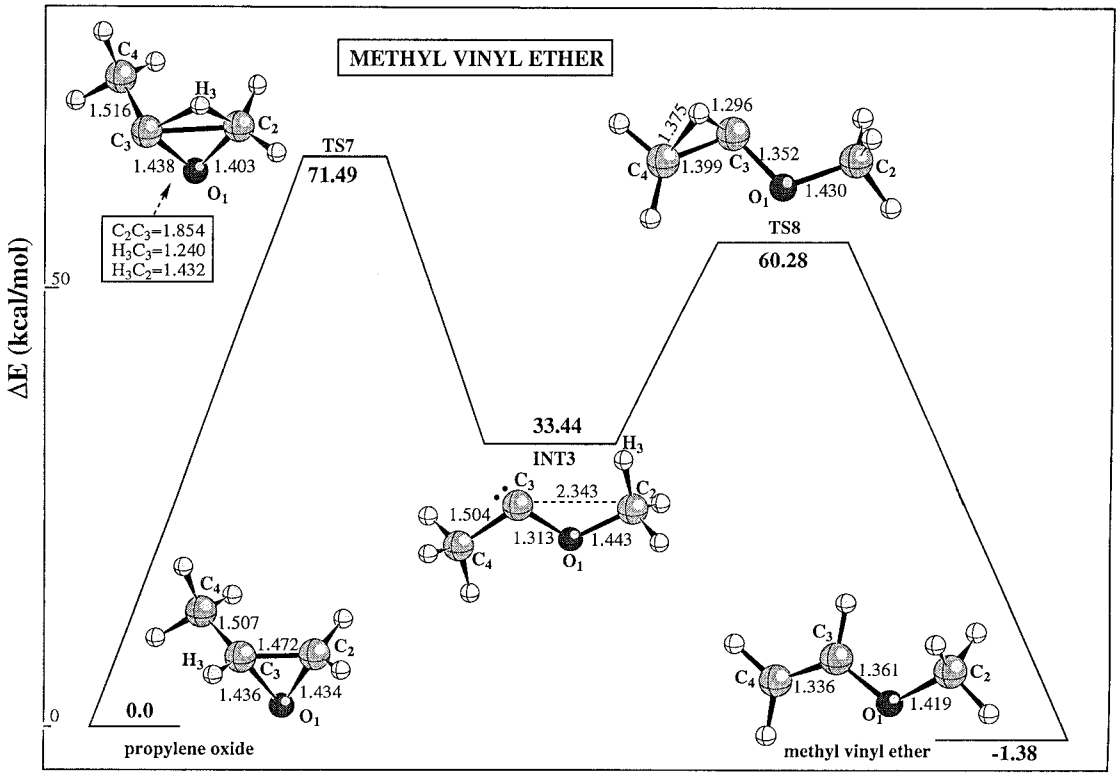

Figure 5. Potential energy profile of the propylene oxide → methyl vinyl ether isomerization via carbene intermediate. Relative energies (in kcal/mol) are calculated at the CCSD(T)//B3LYP/cc-pVDZ level of theory. Distances (in Å) and angles (in degrees) are shown as calculated at the B3LYP level. This path has a much higher barrier than that of the biradical mechanism.

higher than the barrier of the previous surface, and thus it is an unimportant path from a kinetic viewpoint. We were also able to find a path via a triplet carbine intermediate, but its energy barrier was 97.64 kcal/mol at CCSD(T) level, which is even higher than the singlet.

IV. Note on Multireference Effects

We have examined the multireference character of the transition states and intermediates by determining values of T_1, a diagnostic that was introduced by Lee and Taylor[26] to determine the degree of the multireference character. They showed that a T_1 value of 0.02 or greater "indicates a degree of multirefence character large enough to cast a serious doubt on the reliability of a single reference correlation treatment".[27] In this investigation, we have found that among all the calculated species, three transition states had values of T_1 above 0.02. These species were TS1 (acetone), TS2 (propanal), and TS3 (allyl alcohol) with values of 0.091, 0.088, and 0.026, respectively. All of the other species had T_1 values of less than 0.02. However, it has been shown[28−30] that the coupled cluster theory, with the inclusion of perturbative estimates for the effects of triple excitations, can compensate for inadequacies in the single-determinant reference. In view of these findings, we used coupled cluster theory CCSD(T) for configuration interaction calculations at B3LYP geometry.

We have carried out an additional test on the surface of propylene oxide → acetone isomerization, as TS1 had the highest multirefence character, using the complete active space self-consistent-field (CASSCF) level. This enables one to estimate the influence of nondynamical correlation, which was not taken into account using the B3LYP method. The obtained energy barrier was 56.44 kcal/mol at CASSCF(4,3)/cc-pVDZ level with ZPE correction, compared to 54.18 kcal/mol at the CCSD(T)//B3LYP/cc-pVDZ level of theory. The difference is about 2.2 kcal/mol. In our kinetic modeling, which will be described later, we used the values obtained by the CCSD(T)//B3LYP/cc-pVDZ level of theory.

V. Kinetic Modeling

To evaluate the high-pressure limit first-order rate constants from the quantum chemical calculations, the relation

$$k_\infty = \sigma\,(kT/h)\exp(\Delta S^{\#}/R)\exp(-\Delta H^{\#}/RT) \qquad (1)$$

was used,[31,32] where h is Planck constant, k is Boltzmann factor, σ is the degeneracy of the reaction coordinate, and $\Delta H^{\#}$ and $\Delta S^{\#}$ are the enthalpy and entropy of activation, respectively. Because we deal with isomerizations, there is no change in the number of moles $\Delta H^{\#} = \Delta E^{\#}$, where $\Delta E^{\#}$ is the energy difference between the transition state and the reactant. $\Delta E^{\#}$ is equal to $\Delta E^0_{\text{total}} + \Delta(ZPE)$, where $\Delta E^0_{\text{total}}$ is obtained by taking the difference between the total energies of the transition state and the reactant and $\Delta(ZPE)$ is the difference between ZPE of these species. The calculated entropies, zero-point energies, and relative energies $\Delta E^{\#}$ are shown in Table 1. Table 2 summarizes the high-pressure limit rate constants for the four-isomerization reactions based on the values given in Table 1.

In the case of propanal, the two hydrogen atoms on one of the carbon atoms are equivalent in the sense that their distances from the second carbon atom are practically the same, 2.224 and 2.233 Å respectively. Therefore, the degeneracy of the reaction coordinate for the production of propanal, which involves a migration of one of these two hydrogen atoms, is 2. For acetone, only one hydrogen atom can migrate so that $\sigma = 1$. In the reaction coordinate for the production of allyl alcohol, one hydrogen atom migrates from the methyl group to the

TABLE 2: Reaction Schemes for the Propylene Oxide Isomerizations

	reaction	σ^a	$\Delta S^{\#\,b}$	$A_\infty{}^c$ at 1000 K	$E_\infty{}^d$	$\Delta S^o{}_{reaction}{}^b$	$\Delta H^o{}_{reaction}{}^d$
1	propylene oxide → acetone	1	1.04	3.5×10^{13}	54.18	5.28	−32.75
2	propylene oxide → propanal	2	1.94	1.1×10^{14}	54.45	3.85	−25.33
3	propylene oxide → allyl alcohol	2	−1.27	2.2×10^{13}	60.17	1.82	−7.30
4	propylene oxide → methyl vinyl ether (via TS5)	1	3.63	1.3×10^{14}	59.32	1.34	−3.39

[a] Reaction coordinate degeneracy. [b] Entropy of activation and entropy of reaction in cal/(K·mol). [c] Pre-exponential factors in s^{-1}. [d] Activation energy and enthalpy of reaction in kcal/mol.

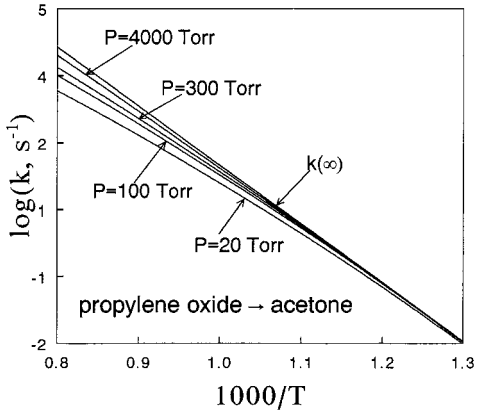

Figure 6. Arrhenius plots of the CCSD(T) calculated rate constants for the propylene oxide → acetone isomerization at different pressures as obtained by RRKM calculations.

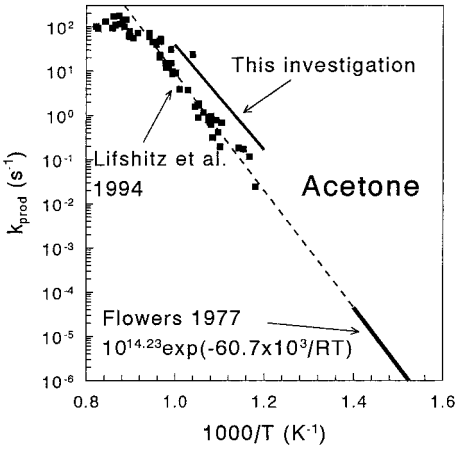

Figure 7. Arrhenius plots of the experimental and calculated rate constants of the propylene oxide → acetone isomerization.

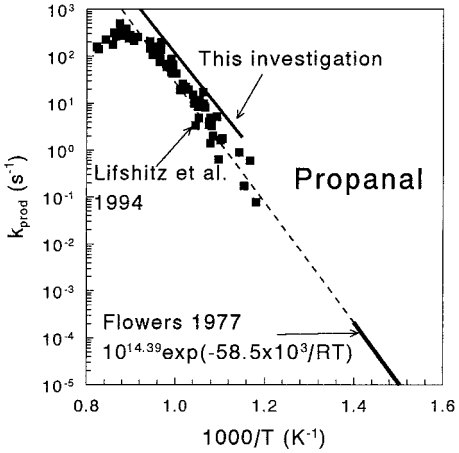

Figure 8. Arrhenius plots of the experimental and calculated rate constants of the propylene oxide → propanal isomerization.

oxygen. Out of the three hydrogen atoms on the methyl group, two are identical in the sense that their distances from the oxygen atom are practically the same (2.789 and 2.922 Å, respectively). The distance of the third hydrogen is longer 3.422 Å. The IRC calculations show that the migration of the hydrogen atom to the oxygen involves only one of the two atoms that are closer to the oxygen. The degeneracy of the reaction coordinate is, therefore, 2. The production of methyl vinyl ether does not involve hydrogen atom migration in the crucial stage, instead it involves only a C−C bond cleavage. There is, therefore, no degeneracy to the reaction coordinate in this reaction.

Figure 6 shows, as an example, RRKM calculations of the propylene oxide → acetone isomerization performed for different temperatures and pressures using the results obtained at the CCSD(T) level of theory. The RRKM calculations employed the standard routine,[33] which uses a direct vibrational state count with classical rotation for the transition state. The threshold energy is 54 180 cal/mol and $< E_{down} > = 600$ cm^{-1}. As can be seen at the temperature range of this investigation and at a pressure of ∼2 atm, the rate constant is practically the high-pressure limit rate constant. In our comparison between the calculations and experiments, we have used the high-pressure limit rate constants.

In view of the fact that two of the decomposition products, acetone ($\Delta H^0_f = -51.9$ kcal/mol) and propanal ($\Delta H^0_f = -44.8$ kcal/mol), are much more stable than propylene oxide ($\Delta H^0_f = -22.6$ kcal/mol),[34] these two isomerization products are formed in thermally exited states, which are high enough to decompose before being collisionally de-excited to the bulk Boltzmann distribution. On the basis of the experimental results,[2] which were obtained under similar conditions as those employed in these calculations, the fraction of the thermally excited acetone that will be de-excited is 69% and propanal 79%. We have thus multiplied the corresponding rate constant by 0.69 and 0.79, respectively. These behaviors do not exist in allyl alcohol and methyl vinyl ether. It should be mentioned that at higher temperatures, the isomerization rates decrease with an increase in temperature. This is an indication that unimolecular decomposition becomes increasingly relevant.

Figures 7−10 show Arrhenius plots of the isomerization rate constants. The filled squares are taken from a shock-tube investigation of the isomerization and decomposition of propylene oxide.[2] The heavy line at the low-temperature end of the figures is taken for comparison from a study by Flowers.[1] The dashed line, which passes through the experimental points, is an extrapolation of the low-temperature experiments.[1] The lines, which are located near the experimental points, are the result of the CCSD(T)//B3LYP/cc-pVDZ calculations. As can be seen, the agreement is fair. It should be indicated that the level of disagreement between the RRKM and the experimental results shown in Figures 7−10 is well expected, and these differences can be well accounted for by a ∼2 kcal/mol uncertainty in the critical energies obtained from CCSD(T)/cc-pVDZ//B3LYP/cc-pVDZ calculations.

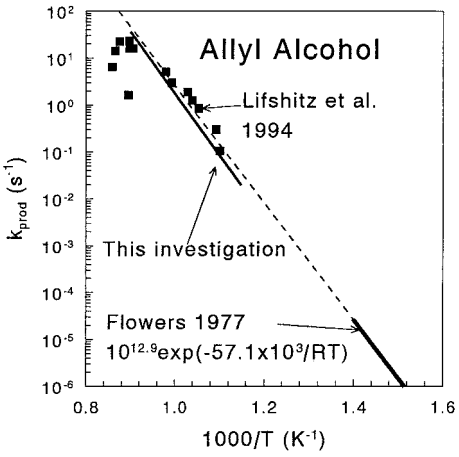

Figure 9. Arrhenius plots of the experimental and calculated rate constants of the propylene oxide → allyl alcohol isomerization.

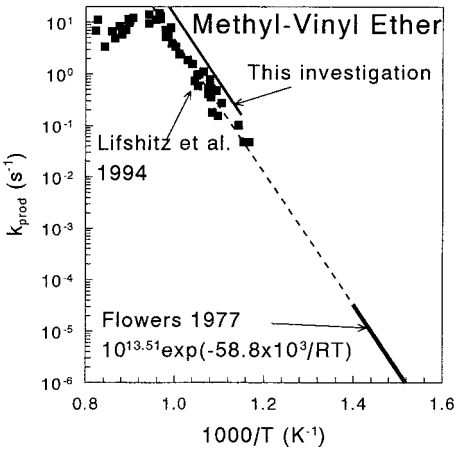

Figure 10. Arrhenius plots of the experimental and calculated rate constants of the propylene oxide → methyl vinyl ether isomerization.

VI. Conclusions

The isomerization of propylene oxide can be summarized by the following features: (1) Three products of the isomerization, acetone, propanal, and allyl alcohol are produced by concerted mechanism. Methyl vinyl ether is formed via stepwise mechanism. (2) Acetone and propanal production are associated with a C−O bond rupture and a 1,2-H-atom shift. The transition states of both products have a closed shell structure. The bond order of the C−O in the transition state is higher than 1, toward the formation of a double bond in the products. (3) The production of allyl alcohol proceeds via a C−O bond rupture and a 1,4-H-atom shift. The transition state is also a closed shell singlet in which the three-membered ring is only partially opened. The transition state is tighter, which expresses itself by a small preexponential factor. (4) The potential energy surface of the isomerization of propylene oxide to methyl vinyl ether contains two intermediates and three transition states. The initial step of the process is a C−C bond cleavage in the ring. Among the three transition states, two have a biradical character and one is a closed shell singlet. The two intermediates are planer, a fact that facilitates the interaction between the unpaired electrons on the carbon atoms and a lone pair of the oxygen, preserving the closed shell structure of both intermediates. The transition state of the cis−trans isomerization (second stage) has the highest energy on the surface and determines the activation energy of the propylene oxide → methyl vinyl ether reaction. (5) Another reaction path for methyl vinyl ether proceeds via a carbene intermediate and has a much higher energy barrier. (6) The rate constants calculated at coupled cluster CCSD(T)//B3LYP/cc-pVDZ level of the theory show a fair agreement with the experimental values.

Acknowledgment. The authors thank the Ministry of Absorption for a fellowship to F.D. in the frame of the Giladi program.

References and Notes

(1) Flowers, M. C. *J. Chem. Soc., Faraday Trans.* **1977**, *73*, 1927.
(2) Lifshitz, A.; Tamburu, C. *J. Phys. Chem.* **1994**, *98*, 1161.
(3) Yamaguchi, Y.; Schaefer, H. F., III.; Alberts I. L. *J. Am. Chem. Soc.* **1993**, *115*, 5790.
(4) Bigot, B.; Sevin, A.; Devaquet, A. *J. Am. Chem. Soc.* **1979**, *101*, 1095.
(5) Knuts, S.; Minaev, B. F.; Vantras, O.; Ågren, H. *Int. J. Quantum Chem.* **1995**, *55*, 23.
(6) Yamaguchi, K.; Yabushita, S.; Fueno, T.; Kato, S.; Morokuma, K. *Chem. Phys. Lett.* **1980**, *70*, 27.
(7) Shinohara, Y.; Mitamura, T.; Nakajiama, T.; Suzuki, S. *Nippon Kagaku Kaishi* **1998**, 643.
(8) Liu, F.; Qi, F.; Gao, H.; Li, C.; Sheng, L.; Zhang, Y.; Yu, S.; Lau, K. C.; Li, W.-K. *J. Phys. Chem.* **1999**, *103*, 4155.
(9) Liu, F.; Sheng, L.; Qi, F.; Gao, H.; Li, C.; Zhang, Y.; Yu, S.; Lau, K.-C.; Li, W.-K. *J. Phys. Chem.* **1999**, *103*, 8179.
(10) Becke, A. D. *J. Chem. Phys.* **1993**, *98*, 5648.
(11) Lee, C.; Yang, W.; Parr, R. G. *Phys. Rev.* **1988**, *B37*, 785.
(12) Dunning, T. H., Jr.; Fabian, J. *Eur. J. Org. Chem.* **1999**, *1107*, 7.
(13) Kendall, R. A.; Dunning, T. H., Jr.; Harrison, R. J. *J. Phys. Chem.* **1992**, *96*, 6796.
(14) Scott, A. P.; Radom, L. *J. Phys. Chem.* **1996**, *100*, 16 502.
(15) Shaik, S. S.; Schlegel, H. B.; Walfe, S. *Theoretical Aspects of Physical Organic Chemistry: the SN2 Mechanism*; Wiley: New York, 1992; p 45.
(16) Sperling, D.; Rei*β*ig, H.-U.; Fabian, J. *Eur. J. Org. Chem.* **1999**, *1107*, 7.
(17) Sperling, D.; Fabian, J. *Eur. J. Org. Chem.* **1999**, *215*, 5.
(18) Houk, K. N.; Nendel, M.; Wiest, O.; Storer, J. M. *J. Am. Chem. Soc.* **1997**, *101*, 1095.
(19) Fan, K.-N.; Li, Z.-H.; Wang, W.-N.; Huang, H.-H.; Huang, W. *Chem. Phys. Lett.* **1997**, *277*, 257.
(20) Skancke, P. N.; Hrovat, D. A.; Borden, W. T. *J. Phys. Chem.* **1999**, *103*, 4043.
(21) Goddard, J. D.; Orlova, G. *J. Chem. Phys.* **1999**, *111*, 7705.
(22) Hess, B. A., Jr.; Eckart, U.; Fabian, J. *J. Am. Chem. Soc.* **1998**, *120*, 12 310.
(23) Brinck, T.; Lee, H.-N.; Jonsson, M. *J. Phys. Chem.* **1999**, *103*, 7094.
(24) Frisch, M. J.; Trucks, G. W.; Schlegel, H. B.; Gill, P. M. W.; Johnson, B. G.; Robb, M. A.; Cheeseman, J. R.; Keith, T.; Petersson, G. A.; Montgomery, J. A.; Rahavachari, K.; Al-Laham, M. A.; Zakrzewski, V. G.; Orviz, J. V.; Foresman, J. B.; Cioslowski, J.; Stefanov, B. B.; Nanayakkara, A.; Challacombe, M.; Peng, C. Y.; Ayala, P. Y.; Chen, W.; Wong, M. W.; Andres, J. L.; Replogle, E. S.; Gomperts, R.; Martin, R. L.; Fox, D. J.; Binkley, J. S.; Defrees, D. J.; Baker, J.; Stewart, J. P.; Head-Gordon, M.; Gonzalez, C.; Pople, J. A. *GAUSSIAN* 94, *Revision* D.4; Gaussian, Inc.: Pittsburgh, 1995.
(25) GAMESS−USA, Revision Mar. 1997; Schmidt, M. W.; Baldridge, K. K.; Boatz, J. A.; Elbert, S. T.; Gordon, M. S.; Jensen, J. H.; Koseki, S.; Matsunaga, N.; Nguyen, K. A.; Su, S. J.; Windus, T. L.; Dupuis, M.; Montgomery, J. A.; Schmidt M. W.; Baldridge, K. K.; Boatz, J. A.; Elbert, S. T.; Gordon, M. S.; Jensen, J. H.; Koseki, S.; Matsunaga, N.; Nguyen, K. A.; Su, S. J.; Windus, T. L.; Dupuis, M.; Montgomery, J. A. *J. Comput. Chem.* **1993**, *14*, 1347.
(26) Lee, T. J.; Taylor, P. R. *Int. J. Quantum Chem. Symp.* **1989**, *23*, 199.
(27) Lee, T. J.; Rendell, A. P.; Taylor, P. R. *J. Phys. Chem.* **1990**, *94*, 5463.
(28) Bartlett, R. J. *J. Phys. Chem.* **1989**, *93*, 1697.
(29) Cramer, C. J.; Nash, J. J.; Squires, R. R. *Chem. Phys. Lett.* **1997**, *277*, 311.
(30) Kraka, E.; Cremer, D. *J. Am. Chem. Soc.* **1994**, *116*, 4929.
(31) Eyring, H. *J. Chem. Phys.* **1935**, 3, 107.
(32) Evans, M. G.; Polanyi, M. *Trans. Faraday Soc.* **1935**, 31, 875.
(33) Kiefer, J. H.; Shah, J. N. *J. Chem. Phys.* **1987**, 91, 3024.
(34) Stein, S. E.; Lias, S. G.; Liebman, J. F.; Levin, R. D.; Kafafi, S. A. *Structures and Properties*. NIST Standard reference database 25. Version 2.01; National Institute of Standards and Technology: Gaitherburg, MD, 1994.